

Half-Heusler Compounds as a New Class of Three-Dimensional Topological Insulators

Di Xiao,¹ Yugui Yao,^{2,3} Wanxiang Feng,² Jun Wen,³ Wenguang Zhu,^{4,1} Xingqiu Chen,¹ G. Malcolm Stocks,¹ and Zhenyu Zhang^{1,4,5}

¹*Materials Science & Technology Division, Oak Ridge National Laboratory, Oak Ridge, TN 37831, USA*

²*Beijing National Laboratory for Condensed Matter Physics and Institute of Physics, Chinese Academy of Sciences, Beijing 100190, China*

³*Department of Physics, The University of Texas at Austin, Austin, TX 78712, USA*

⁴*Department of Physics and Astronomy, The University of Tennessee, Knoxville, TN 37996, USA*

⁵*ICQD, University of Science and Technology of China, Hefei, Anhui, 230026, China*

Using first-principles calculations within density functional theory, we explore the feasibility of converting ternary half-Heusler compounds into a new class of three-dimensional topological insulators (3DTI). We demonstrate that the electronic structure of unstrained LaPtBi as a prototype system exhibits distinct band-inversion feature. The 3DTI phase is realized by applying a uniaxial strain along the [001] direction, which opens a bandgap while preserving the inverted band order. A definitive proof of the strained LaPtBi as a 3DTI is provided by directly calculating the topological \mathbb{Z}_2 invariants in systems without inversion symmetry. We discuss the implications of the present study to other half-Heusler compounds as 3DTI, which, together with the magnetic and superconducting properties of these materials, may provide a rich platform for novel quantum phenomena.

PACS numbers: 71.15.Dx, 71.18.+y, 73.20.At, 73.61.Le

Recent years have seen a surge of interest in a new class of materials called topological insulators [1–3]. These materials are distinguished from ordinary insulators by nontrivial topological invariants associated with the bulk electronic structure [4–6]. The existence of the topological invariants dictates that the excitation gap must vanish at the boundaries of a topological insulator, resulting in the formation of robust metallic surface states. A number of spectacular quantum phenomena have been predicted when the surface states are under the influence of magnetism and superconductivity [7–11]. To fully explore these phenomena thus demands great versatility from the host material. However, so far the experimental realizations of topological insulators are limited to a few classes of simple materials, including HgTe quantum well [12, 13], Bi_{1-x}Sb_x alloy [14, 15], and tetradymite semiconductors such as Bi₂Se₃, Bi₂Te₃, and Sb₂Te₃ [16–18]. Realizing the necessary conditions for the predicted phenomena in these materials can be difficult.

The search for topological insulators has greatly benefited from the topological band theory. It has been shown that for all known topological insulators, in addition to the strong spin-orbit coupling, their electronic structure can be characterized by a band-inversion which involves the switching of bands with opposite parity around the Fermi level [12, 14, 16]. This is very similar to the quantum Hall effect in which two bands are allowed to exchange their Chern numbers only when they come into contact with each other [19]. The above observation suggests small bandgap semiconductors or semimetals with heavy elements as promising candidates as these materials are likely to develop an inverted band order.

In this Letter we predict a new class of topological in-

ulators realized in small bandgap ternary half-Heusler compounds [20]. In particular, using first-principles calculations we demonstrate that LaPtBi as a prototype system becomes a strong topological insulator upon the application of a uniaxial strain along the [001] direction. This result is first discussed using the aforementioned band-inversion mechanism, then verified by direct calculation of the \mathbb{Z}_2 topological invariants from the bulk band structure [21, 22]. Remarkably, ternary half-Heusler compounds already boast an impressive list of the much desired properties such as magnetism [23] and superconductivity [24]. Together with the predicted topological properties, these materials provide an exciting platform for novel quantum phenomena.

Ternary half-Heusler compounds have the chemical formula XYZ , where X and Y are transition or rare earth

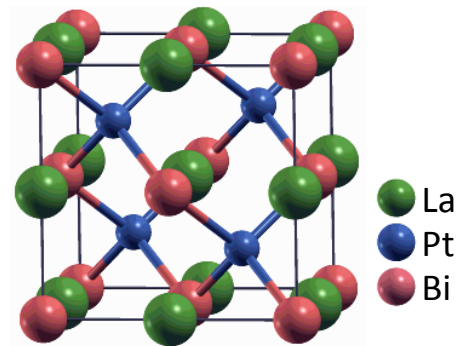


FIG. 1: (color online) Crystal structure of half-Heusler compound LaPtBi in the $F\bar{4}3m$ space group. Green spheres at (0.5,0.5,0.5) are atom La, dark blue spheres at (0.25,0.25,0.25) are atom Pt, and pink spheres at (0,0,0) are atom Bi.

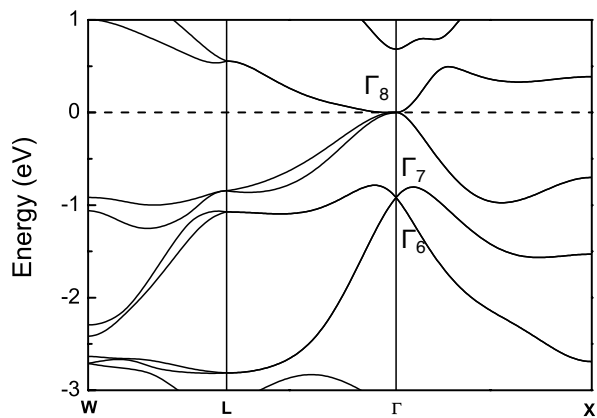


FIG. 2: Band structure of LaPtBi with experimental lattice constant $a=6.83$ Å. The band order at the Γ point is Γ_8 , Γ_7 , and Γ_6 in descendent order of energy. There is a small gap between the Γ_7 and Γ_6 states.

metals and Z a heavy element. Figure 1 shows the crystal structure of LaPtBi, which consists of three interpenetrating, face-centered-cubic lattices with Pt sitting at the unique site. It can be regarded as a hybrid compound of LaBi with the rock-salt structure, and LaPt and PtBi with the zinc-blende structure. Unlike tetradymite semiconductors, the spatial inversion symmetry is broken in half-Heusler structure.

When the total valence electron count in a primitive unit cell is 18, the half-Heusler compounds are expected to have a band gap. However, some compounds display a distinctive semimetal behavior with LaPtBi being one of the examples [32]. To investigate the band topology, we employ the full-potential linearized augmented plane-wave method [26] with the local spin density approximation for the exchange-correlation potential [27]. Fully relativistic band calculations were performed using the program package WIEN2K [28]. A converged ground state was obtained using 10,000 k points in the first Brillouin zone and $K_{\max}R_{MT} = 9$, where R_{MT} represents the muffin-tin radius and K_{\max} the maximum size of the reciprocal-lattice vectors. Wave functions and potentials inside the atomic sphere are expanded in spherical harmonics up to $l = 10$ and 4, respectively. Spin orbit coupling are included by a second-variational procedure [26], where states up to 9 Ry above Fermi energy are included in the basis expansion, and the relativistic $p_{1/2}$ corrections were also considered for 5p, 6p of Pt, and 6p of Bi in order to improve the accuracy [29, 30]. The calculations were performed using the experimental lattice constant of 6.83 Å [31]. Figure 2 shows the fully relativistic energy band structure of LaPtBi. As anticipated from experiments [32], LaPtBi is a semimetal with very small electron and hole pockets around the Γ point. Our result is consistent with previous calculations [25].

As already pointed out by Ogüchi [25], the band

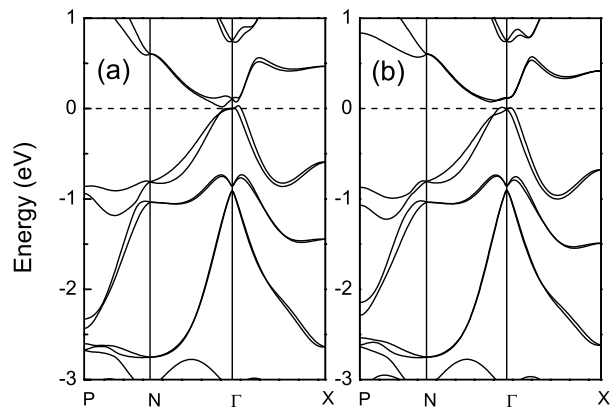


FIG. 3: Band structure of LaPtBi under uniaxial strain with constant volume along [001]-direction, reduce the c/a ratio by 5% in (a), and increase the c/a ratio by 5% in (b).

structure near the Fermi level at the Γ point is determined mainly by PtBi with the zinc-blende structure, and the La states participate in the band structure additively. This separation allows us to draw direct comparison with a known topologically nontrivial compound HgTe [12, 14], which is a II-VI material also with the zinc-blende structure. Let us focus on the bands at the Γ point close to the Fermi level. Similar to the case of HgTe, symmetry analysis shows that the fourfold degenerate Γ_8 states lies above the twofold degenerate Γ_7 and Γ_6 states. As discussed by Fu and Kane [14], such a band inversion is a strong indication that LaPtBi is in a topologically nontrivial state. To remove the semi-metallic behavior, we apply a uniaxial strain along the [001] direction with constant volume to break the fourfold degeneracy of the Γ_8 states. Figure 3 shows the resulting band structure. We find that although a local bandgap can be opened, the system responds differently to compression and elongation: Upon compression the material remains a semimetal while it becomes an insulator when stretched. The inverted band order stays the same. For comparison, we also calculated the band structure with hydrostatic strain, shown in Fig. 4. A global band gap is opened by the hydrostatic strain when the lattice is compressed while the semi-metallic behavior is retained with expansion. However, in the former case the Γ_6 states now jumps above the Γ_8 states with the Fermi energy lies in between. In this situation, the material should be in a topologically trivial phase.

Although the band inversion near the Γ point is a strong indication that LaPtBi under uniaxial strain is in a topologically insulating phase, it is not definitive because the topological invariant is a global property of the entire Brillouin zone. Fu and Kane have proposed a parity criterion to identify topological insulators in systems with both time-reversal and spatial inversion symmetry [14]. However, it cannot be applied here because of

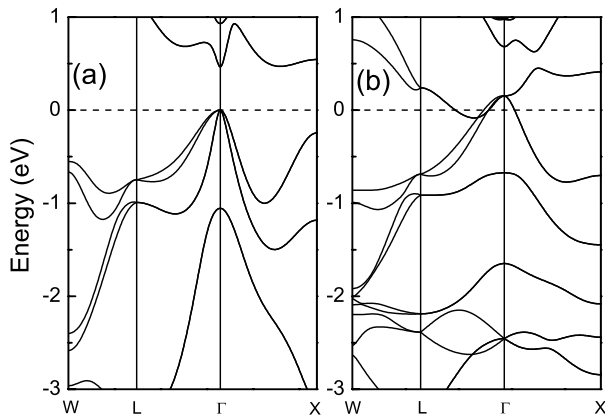


FIG. 4: Band structure of LaPtBi under hydrostatic strain, $a=a-7\%a$ in (a), $a=a+7\%a$ in (b)

the lack of inversion symmetry in the half-Heusler structure. Instead, we calculate the topological invariants directly from the bulk band structure.

We first briefly describe the formalism for a 2D system. In the presence of time-reversal symmetry, Kramer's theorem dictates that the energy eigenstates must come in pairs. This allows us to enforce the so-called time-reversal constraint on the Bloch functions:

$$|u_n(-\mathbf{k})\rangle = \Theta|u_n(\mathbf{k})\rangle, \quad (1)$$

where $|u_n(\mathbf{k})\rangle$ is the periodic part of the Bloch function, and $\Theta = e^{i\pi S_y/\hbar}K$ is the time reversal operator with S_y the spin operator and K the complex conjugation. Accordingly, we only need to obtain Bloch functions in half of the Brillouin zone, denoted by \mathcal{B}^+ , as those in the other half are fixed by Eq. (1). The band topology is characterized by the \mathbb{Z}_2 invariant, given by [21]

$$\mathbb{Z}_2 = \frac{1}{2\pi} \left[\oint_{\partial\mathcal{B}^+} d\mathbf{k} \cdot \mathcal{A}(\mathbf{k}) - \int_{\mathcal{B}^+} d^2k \mathcal{F}(\mathbf{k}) \right] \text{ mod } 2, \quad (2)$$

where $\mathcal{A}(\mathbf{k}) = i \sum_n \langle u_n(\mathbf{k}) | \nabla_{\mathbf{k}} u_n(\mathbf{k}) \rangle$ is the Berry connection and $\mathcal{F}(\mathbf{k}) = \nabla_{\mathbf{k}} \times \mathcal{A}(\mathbf{k})|_z$ is the Berry curvature; the sum is over occupied bands. A topological insulator is characterized by $\mathbb{Z}_2 = 1$ while ordinary insulators have $\mathbb{Z}_2 = 0$. The nonzero \mathbb{Z}_2 invariant is an obstruction to smoothly defining the Bloch functions in \mathcal{B}^+ under the time-reversal constraint.

To numerically perform the integration, we follow the recipe by Fukui and Hatsugai [22]. The Bloch functions $|u_n(\mathbf{k})\rangle$ are first obtained on a \mathbf{k} -space mesh in \mathcal{B}^+ . The mesh must include the four time-reversal invariant \mathbf{k} -points: $\mathbf{0}$, $\mathbf{G}_1/2$, $\mathbf{G}_2/2$ and $(\mathbf{G}_1 + \mathbf{G}_2)/2$, expressed in terms of the reciprocal lattice vectors. After applying the time-reversal constraint, next we introduce the link variable central to many Berry-phase related calculations [33, 34], given by $U_{\boldsymbol{\mu}}(\mathbf{k}_j) = \det \langle |u_n(\mathbf{k}_j)\rangle | u_m(\mathbf{k}_j + \boldsymbol{\mu}) \rangle \rangle$, where $\boldsymbol{\mu}$ is the unit vector on the mesh, and n and

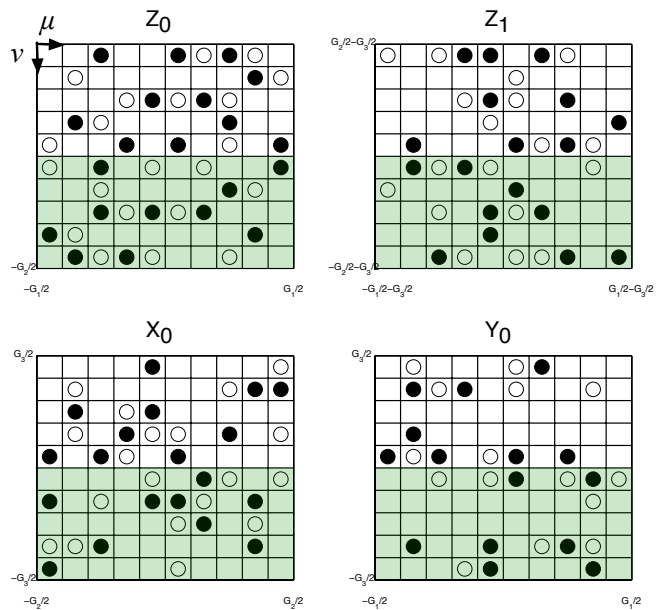


FIG. 5: The n -field configuration for LaPtBi under uniaxial strain computed under the time-reversal constraint. The four tori are Z_0 , Z_1 , X_0 and Y_0 with the shaded area indicating half of the area. $\boldsymbol{\mu}$ and $\boldsymbol{\nu}$ are the unit vectors of the \mathbf{k} -space mesh. The white and black circles denote $n = 1$ and -1 , respectively, while the blank denotes 0. The \mathbb{Z}_2 invariant for each individual tori is obtained by summing the n -field over half of the tori. These read $z_0 = 1$, $z_1 = 0$, $x_0 = 1$, and $y_0 = 1$. The \mathbb{Z}_2 invariants of the system are $1; (000)$.

m run through occupied bands. The finite element expressions for \mathcal{A} and \mathcal{F} are $\mathcal{A}_{\boldsymbol{\mu}}(\mathbf{k}_j) = \text{Im} \log U_{\boldsymbol{\mu}}(\mathbf{k}_j)$, and $\mathcal{F}(\mathbf{k}_j) = \text{Im} \log U_{\boldsymbol{\mu}}(\mathbf{k}_j) U_{\boldsymbol{\nu}}(\mathbf{k}_j + \boldsymbol{\mu}) U_{\boldsymbol{\mu}}^{-1}(\mathbf{k}_j + \boldsymbol{\nu}) U_{\boldsymbol{\nu}}^{-1}(\mathbf{k}_j)$, where the return value of the complex logarithm function is confined to its principal branch $(-\pi, \pi]$. We can then insert these expressions into Eq. (2) to calculate the \mathbb{Z}_2 invariant. Define an integer field $n(\mathbf{k}_j)$ for each plaquette:

$$n(\mathbf{k}_j) = \frac{1}{2\pi} \left\{ [\Delta_{\boldsymbol{\nu}} \mathcal{A}_{\boldsymbol{\mu}}(\mathbf{k}_j) - \Delta_{\boldsymbol{\mu}} \mathcal{A}_{\boldsymbol{\nu}}(\mathbf{k}_j)] - \mathcal{F}(\mathbf{k}_j) \right\}, \quad (3)$$

where $\Delta_{\boldsymbol{\mu}}$ is the forward difference operator. The \mathbb{Z}_2 invariant is given by the sum of the n -field in half of the Brillouin zone [22], i.e., $\mathbb{Z}_2 = \sum_{\mathbf{k}_j \in \mathcal{B}^+} n(\mathbf{k}_j) \text{ mod } 2$.

In 3D the topology of the bands are characterized by four independent \mathbb{Z}_2 invariants [4, 5]. These can be computed by considering six tori in the Brillouin zone. For example, the torus Z_0 is spanned by \mathbf{G}_1 and \mathbf{G}_2 with the third component fixed at 0, and Z_1 is obtained by fixing the third component at $\mathbf{G}_3/2$. The other four tori X_0 , X_1 , Y_0 , and Y_1 are defined similarly. For each torus, one can calculate the corresponding \mathbb{Z}_2 invariant using the steps outlined above for 2D systems. Out of the six possible \mathbb{Z}_2 invariants only four of them are independent. Following Ref. [4, 5], we use the notation $\nu_0; (\nu_1 \nu_2 \nu_3)$, with $\nu_0 = (z_0 + z_1) \text{ mod } 2$, $\nu_1 = x_1$, $\nu_2 = y_1$ and $\nu_3 = z_1$,

where z_0 is the \mathbb{Z}_2 invariant associated with the 2D torus Z_0 . The other \mathbb{Z}_2 invariants are defined similarly. A nonzero ν_0 indicates that the system is a strong topological insulator.

Figure 5 shows the n -field configuration for LaPtBi under uniaxial strain from first-principles calculations. The corresponding band structure is shown in Fig. 3(b). Note that although the n -field itself depends on the gauge choice, their sum over half of the Brillouin zone is gauge-invariant module 2. [38] We find that LaPtBi under uniaxial strain becomes a strong topological insulator with the topological invariants 1;(000). However, under hydrostatic strain [Fig. 4(a)], LaPtBi becomes an ordinary insulator. Furthermore, although the band structure in Fig. 3(a) shows a semi-metallic phase, we can still calculate the \mathbb{Z}_2 invariants for the bands because a local energy gap separates the conduction and valance bands throughout the Brillouin zone. In this case, LaPtBi becomes a topological metal with $\nu_0 = 1$.

Having firmly established that LaPtBi under uniaxial strain realizes a topological insulating phase, we have calculated a number of other half-Heusler ternary compounds by first-principles method. We find that LuPtSb, ScPtBi, YPdBi, YPtSb have inverted band structure, and the 3DTI phase can be induced by uniaxial strain along [001]-direction. Generally, for many small bandgap half-Heusler compounds, the topologically insulating phase can be realized by a combination of hydrostatic strain to change the band order and uniaxial strain to open an energy gap. Details of the first-principles calculations will be reported elsewhere [35].

In conclusion, we have shown that the 18-electron ternary half-Heusler compounds can be tuned into a new class of three-dimensional topological insulators via proper strain engineering. This is confirmed by first-principles calculation of the topological \mathbb{Z}_2 invariants in systems without inversion symmetry. This quantum nature, plus other interesting physical properties of these materials, such as magnetism [23] and superconductivity [24], characterize these materials as an exciting platform for novel quantum phenomena.

Note added: After the completion of the bulk of this work (see, e.g., the brief announcement in Ref. [20]), two more related studies have appeared [36, 37], confirming and expanding the predictions of the present work.

DX acknowledges useful discussions with Ying Ran. This work was supported by the Division of Materials Sciences and Engineering, Office of Basic Energy Sciences, U.S. Department of Energy, by NSF of China (10674163, 10974231), the MOST Project of China (2006CB921300, 2007CB925000), and by Welch Foundation (F-1255).

- [2] M. Z. Hasan and C. L. Kane, arXiv:1002.3895.
- [3] J. E. Moore, Nature **464**, 194 (2010).
- [4] J. E. Moore and L. Balents, Phys. Rev. B **75**, 121306 (2007).
- [5] L. Fu, C. L. Kane, and E. J. Mele, Phys. Rev. Lett. **98**, 106803 (2007).
- [6] R. Roy, Phys. Rev. B **79**, 195322 (2009).
- [7] X.-L. Qi, T. L. Hughes, and S.-C. Zhang, Phys. Rev. B **78**, 195424 (2008).
- [8] L. Fu and C. L. Kane, Phys. Rev. Lett. **100**, 096407 (2008).
- [9] L. Fu and C. L. Kane, Phys. Rev. Lett. **102**, 216403 (2009).
- [10] Y. Tanaka, T. Yokoyama, and N. Nagaosa, Phys. Rev. Lett. **103**, 107002 (2009).
- [11] T. Yokoyama, J. Zang, and N. Nagaosa, arXiv:1003.3769.
- [12] B. A. Bernevig, T. L. Hughes, and S.-C. Zhang, Science **314**, 1757 (2006).
- [13] M. König *et al.*, Science **318**, 766 (2007).
- [14] L. Fu and C. L. Kane, Phys. Rev. B **76**, 045302 (2007).
- [15] D. Hsieh *et al.*, Nature **452**, 970 (2008).
- [16] H. Zhang *et al.*, Nat. Phys. **5**, 438 (2009).
- [17] Y. Xia *et al.*, Nat. Phys. **5**, 398 (2009).
- [18] Y. L. Chen *et al.*, Science **325**, 178 (2009).
- [19] J. E. Avron, R. Seiler, and B. Simon, Phys. Rev. Lett. **51**, 51 (1983).
- [20] D. Xiao *et al.*, *Three dimensional topological insulators on the half-Heusler lattice*, Bulletin of the American Physical Society, 2010 March Meeting, URL <http://meetings.aps.org/link/BAPS.2010.MAR.Q38.1>.
- [21] L. Fu and C. L. Kane, Phys. Rev. B **74**, 195312 (2006).
- [22] T. Fukui and Y. Hatsugai, J. Phys. Soc. Jpn. **76**, 053702 (2007).
- [23] P. C. Canfield *et al.*, J. Appl. Phys. **70**, 5800 (1991).
- [24] G. Goll *et al.*, Physica B: Condensed Matter **403**, 1065 (2008).
- [25] T. Oguchi, Phys. Rev. B **63**, 125115 (2001). The band structure was calculated using the lattice constant 6.867 Å reported in Ref. [32].
- [26] D. J. Singh, *Pseudopotentials and the LAPW Method* (Kluwer Academic, Boston, 1994).
- [27] J. P. Perdew and Y. Wang, Phys. Rev. B **45**, 13244 (1992).
- [28] P. Blaha, K. Schwarz, G. Madsen, D. Kvaniscka, and J. Luitz, *Wien2k, An Augmented Plane Wave Plus Local Orbitals Program for Calculating Crystal Properties* (Vienna University of Technology, Vienna, Austria, 2001).
- [29] J. Kunes, P. Novak, R. Schmid, P. Blaha, and K. Schwarz, Phys. Rev. B **64**, 153102 (2001).
- [30] P. Larson, Phys. Rev. B **68**, 155121 (2003).
- [31] M. G. Haase *et al.*, J. of Solid State Chem. **168**, 18 (2002).
- [32] M. H. Jung *et al.*, J. Appl. Phys. **89**, 7631 (2001).
- [33] R. D. King-Smith and D. Vanderbilt, Phys. Rev. B **47**, 1651 (1993).
- [34] R. Resta, Rev. Mod. Phys. **66**, 899 (1994).
- [35] Y. Yao *et al.*, in preparation.
- [36] H. Lin *et al.*, Nature Mater. **9**, 546 (2010).
- [37] S. Chadov *et al.*, Nature Mater. **9**, 541 (2010).
- [38] The sum of n -field over the entire Brillouin zone gives the Chern number, which vanishes identically for time-reversal invariant systems.